

Phase diagram of underdoped cuprate superconductors: effect of Cooper-pair phase fluctuations

C. Timm,* D. Manske, and K. H. Bennemann

Institut für Theoretische Physik, Freie Universität Berlin, Arnimallee 14, D-14195 Berlin, Germany

(Dated: February 16, 2002)

In underdoped cuprates fluctuations of the phase of the superconducting order parameter play a role due to the small superfluid density. We consider the effects of phase fluctuations assuming the exchange of spin fluctuations to be the predominant pairing interaction. Spin fluctuations are treated in the fluctuation-exchange approximation, while phase fluctuations are included by Berezinskii-Kosterlitz-Thouless theory. We calculate the stiffness against phase fluctuations, $n_s(\omega)/m^*$, as a function of doping, temperature, and frequency, taking its renormalization by phase fluctuations into account. The results are compared with recent measurements of the high-frequency conductivity. Furthermore, we obtain the temperature T^* , where the density of states at the Fermi energy starts to be suppressed, the temperature T_c^* , where Cooper pairs form, and the superconducting transition temperature T_c , where their phase becomes coherent. We find a crossover from a phase-fluctuation-dominated regime with $T_c \propto n_s$ for underdoped cuprates to a BCS-like regime for overdoped materials.

PACS numbers: 74.20.Mn, 74.40.+k, 74.72.-h

I. INTRODUCTION

For about fifteen years cuprate high-temperature superconductors (HTSC's) have stimulated significant advances in the theory of highly correlated systems as well as in soft condensed matter theory. Nevertheless, we still do not fully understand the various phases of these materials. Of particular interest is the underdoped regime of hole-doped cuprates, in which the hole density (doping) x in the CuO_2 planes is lower than required for the maximum superconducting transition temperature T_c . In this regime the superfluid density n_s decreases with decreasing doping and is found to be proportional to T_c .¹ Above T_c , one finds a strong suppression of the electronic density of states close to the Fermi energy, *i.e.*, a *pseudogap*, which appears to have the same symmetry as the superconducting gap.² Furthermore, there may be fluctuating charge and spin modulations (stripes).³

It has been recognized early on that the small superfluid density n_s leads to a reduced stiffness against fluctuations of the phase of the superconducting order parameter.^{4,5,6} Phase fluctuations are additionally enhanced because they are canonically conjugate to charge density fluctuations, which are believed to be suppressed.^{4,6} Furthermore, the cuprates consist of weakly coupled two-dimensional (2D) CuO_2 planes so that fluctuations are enhanced by the reduced dimensionality. Phase fluctuations might destroy the long-range superconducting order, although there is still a condensate of preformed Cooper pairs. In conventional, bulk superconductors this mechanism is not relevant, since the large superfluid density leads to a typical energy scale of phase fluctuations much higher than the superconducting energy gap Δ , which governs the thermal breaking of Cooper pairs. Thus in conventional superconductors the transition is due to the destruction of the Cooper pairs and T_c is proportional to Δ .⁷ On the other hand,

the observation that $T_c \propto n_s$ in underdoped cuprates¹ indicates that the phase fluctuations drive the transition in this regime. The Cooper pairs only break up at a crossover around $T_c^* > T_c$. If the feedback of phase fluctuations on the local formation of Cooper pairs is small, T_c^* is approximately given by the transition temperature one would obtain without phase fluctuations. Between T_c and T_c^* Cooper pairs exist but the order parameter is not phase coherent.^{4,5,6,8,9} Recent thermal-expansion experiments strongly support this picture.¹⁰ However, there is no close relation between our T_c^* and the mean-field transition temperature of Ref. 10, which is determined by extrapolation from the low- T behavior of the expansivity.

There is a third temperature scale T^* with $T^* > T_c^*$, below which a pseudogap starts to open up as seen in nuclear magnetic resonance, tunneling, and transport experiments.^{11,12,13,14,15} It seems unlikely that the pseudogap at these temperatures is due to local superconductivity. Rather, it is thought to be caused by spin fluctuations⁹ or the onset of stripe inhomogeneities.^{16,17} Recent experiments on the Hall effect in $\text{GdBa}_2\text{Cu}_3\text{O}_{7-\delta}$ films¹⁸ also support the existence of *two* crossover temperatures T_c^* and T^* . In this work we are mostly concerned with the strong pseudogap regime $T_c < T < T_c^*$.

Due to the layered structure of the cuprates, they behave like the 2D XY model except in a narrow critical range around T_c , where they show three-dimensional (3D) XY critical behavior.^{19,20} The standard theory for the 2D XY model, the Berezinskii-Kosterlitz-Thouless (BKT) renormalization group theory,^{21,22,23,24} should thus describe these materials outside of the narrow critical range.^{25,26,27,28,29,30} Also, recent transport measurements for a gate-doped cuprate³¹ with only a single superconducting CuO_2 plane show essentially the same doping dependence of T_c as found for bulk materials. BKT theory predicts a transition at a temperature $T_c <$

T_c^* , due to the unbinding of fluctuating vortex-antivortex pairs in the superconducting order parameter. Gaussian phase fluctuations are less important, since they do not shift T_c .³² In addition, the coupling of the phase to the electromagnetic field causes them to be gapped at the plasma frequency,³³ whereas the BKT picture of vortex unbinding remains basically unchanged.³⁴

In the early days of HTSC's, BKT theory was invoked to interpret a number of experiments on bulk samples.^{35,36,37,38,39,40} Recently, two experiments have lent strong additional support to the BKT description: First, Corson *et al.*⁴¹ have measured the complex conductivity of underdoped $\text{Bi}_2\text{Sr}_2\text{CaCu}_2\text{O}_{8+\delta}$ and extracted the frequency-dependent phase stiffness from the data. The authors interpret their data in terms of dynamical vortex-pair fluctuations^{23,42} and conclude that vortices—and thus a local superconducting condensate—exist up to at least 100 K. We discuss this assertion in Sec. III. Second, Xu *et al.*⁴³ have found signs of vortices at temperatures much higher than T_c in underdoped $\text{La}_{2-x}\text{Sr}_x\text{CuO}_4$ in measurements of the Nernst effect. A recent reanalysis of the data⁴⁴ yields an onset temperature of vortex effects of 40 K for an extremely underdoped sample ($x = 0.05$) and of 90 K for $x = 0.07$.

So far, we have not said anything about the superconducting pairing mechanism. There is increasing evidence that pairing is mainly due to the exchange of spin fluctuations. The conserving fluctuation-exchange (FLEX) approximation^{9,45,46,47,48,49} based on this mechanism describes optimally doped and overdoped cuprates rather well. In particular, the correct doping dependence and order of magnitude of T_c are obtained in this regime. On the other hand, the FLEX approximation does not include phase fluctuations and we believe this to be the main reason why it fails to predict the downturn of T_c in the underdoped regime. Instead, T_c is found to approximately saturate for small doping x . However, the FLEX approximation is able to reproduce two other salient features of underdoped cuprates, namely the decrease of n_s and the opening of a weak pseudogap at T^* , as we show below.

This encourages us to apply the following description. We employ the FLEX approximation to obtain the dynamical phase stiffness $n_s(\omega)/m^*$, where $n_s(\omega)$ is the generalization of the superfluid density for finite frequencies. The static density $n_s(0)$ starts to deviate from zero at the temperature where Cooper pairs start to form and which we identify with T_c^* . Then, phase fluctuations are incorporated by using the phase stiffness from FLEX as the input for BKT theory, which leads to a renormalized $n_s^R < n_s$ and predicts a reduced T_c . Then, we consider the dynamical case $\omega > 0$ and use dynamical BKT theory^{23,42} to find the renormalized phase stiffness $n_s^R(\omega)/m^*$ and compare the results with experiments.⁴¹

II. STATIC CASE

Transport measurements for a gate-doped cuprate³¹ show that the superconducting properties are determined by a single CuO_2 plane. The simplest model believed to contain the relevant strong correlations is the 2D one-band Hubbard model.⁵⁰ We here start from the Hamiltonian

$$H = - \sum_{\langle ij \rangle \sigma} t_{ij} \left(c_{i\sigma}^\dagger c_{j\sigma} + c_{j\sigma}^\dagger c_{i\sigma} \right) + U \sum_i n_{i\uparrow} n_{i\downarrow}. \quad (1)$$

Here, $c_{i\sigma}^\dagger$ creates an electron with spin σ on site i , U denotes the on-site Coulomb interaction, and t_{ij} is the hopping integral. Within a conserving approximation, the one-electron self-energy is given by the functional derivative of a generating functional Φ , which is related to the free energy, with respect to the dressed one-electron Green function \mathcal{G} , $\Sigma = \delta\Phi[H]/\delta\mathcal{G}$.⁵¹ On the other hand, the dressed Green function is given by the usual Dyson equation $\mathcal{G}^{-1} = \mathcal{G}_0^{-1} - \Sigma$ in terms of the unperturbed Green function \mathcal{G}_0 of the kinetic part of H alone. These equations determine the dressed Green function.⁵¹

The T -matrix⁵² or FLEX approximation^{9,45,46,47,48,49} is distinguished by the choice of a particular infinite subset of ladder and bubble diagrams for the generating functional Φ . The dressed Green functions are used to calculate the charge and spin susceptibilities. From these a Berk-Schrieffer-type⁵³ pairing interaction is constructed, describing the exchange of charge and spin fluctuations. In a purely electronic pairing theory a self-consistent description is required because the electrons do not only form Cooper pairs but also mediate the pairing interaction. The quasiparticle self-energy components X_ν ($\nu = 0, 3, 1$) with respect to the Pauli matrices τ_ν in the Nambu representation,^{7,54} *i.e.*, $X_0 = \omega(1 - Z)$ (renormalization), $X_3 = \xi$ (energy shift), and $X_1 = \phi$ (gap parameter) are given by

$$X_\nu(\mathbf{k}, \omega) = \frac{1}{N} \sum_{\mathbf{k}'} \int_0^\infty d\Omega [P_s(\mathbf{k}-\mathbf{k}', \Omega) \pm P_c(\mathbf{k}-\mathbf{k}', \Omega)] \times \int_{-\infty}^\infty d\omega' I(\omega, \Omega, \omega') A_\nu(\mathbf{k}', \omega'). \quad (2)$$

Here, the plus sign holds for X_0 and X_3 and the minus sign for X_1 . The kernel I and the spectral functions A_ν are given by

$$I(\omega, \Omega, \omega') = \frac{f(-\omega') + b(\Omega)}{\omega + i\delta - \Omega - \omega'} + \frac{f(\omega') + b(\Omega)}{\omega + i\delta + \Omega - \omega'}, \quad (3)$$

$$A_\nu(\mathbf{k}, \omega) = -\frac{1}{\pi} \text{Im} \frac{a_\nu(\mathbf{k}, \omega)}{D(\mathbf{k}, \omega)}, \quad (4)$$

where $a_0 = \omega Z$, $a_3 = \epsilon_{\mathbf{k}} + \xi$, $a_1 = \phi$, and

$$D = (\omega Z)^2 - [\epsilon_{\mathbf{k}} + \xi]^2 - \phi^2. \quad (5)$$

Here, f and b are the Fermi and Bose distribution function, respectively. We use the bare tight-binding dispersion relation for lattice constant $a = b = 1$,

$$\epsilon_{\mathbf{k}} = 2t(2 - \cos k_x - \cos k_y - \mu). \quad (6)$$

The band filling $n = 1/N \sum_{\mathbf{k}} n_{\mathbf{k}}$ is determined with the help of the \mathbf{k} -dependent occupation number $n_{\mathbf{k}} = 2 \int_{-\infty}^{\infty} d\omega f(\omega) N(\mathbf{k}, \omega)$ which is calculated self-consistently. $n = 1$ corresponds to half filling. The interactions due to spin and charge fluctuations are given by $P_s = (2\pi)^{-1} U^2 \text{Im} (3\chi_s - \chi_{s0})$ with $\chi_s = \chi_{s0} (1 - U\chi_{s0})^{-1}$ and $P_c = (2\pi)^{-1} U^2 \text{Im} (3\chi_c - \chi_{c0})$ with $\chi_c = \chi_{c0} (1 + U\chi_{c0})^{-1}$. In terms of spectral functions one has

$$\begin{aligned} \text{Im} \chi_{s0,c0}(\mathbf{q}, \omega) &= \frac{\pi}{N} \int_{-\infty}^{\infty} d\omega' [f(\omega') - f(\omega' + \omega)] \\ &\times \sum_{\mathbf{k}} [N(\mathbf{k} + \mathbf{q}, \omega' + \omega) N(\mathbf{k}, \omega') \\ &\pm A_1(\mathbf{k} + \mathbf{q}, \omega' + \omega) A_1(\mathbf{k}, \omega')]. \end{aligned} \quad (7)$$

Here, $N(\mathbf{k}, \omega) = A_0(\mathbf{k}, \omega) + A_3(\mathbf{k}, \omega)$, and the real parts are calculated with the help of the Kramers-Kronig relation. The subtracted terms in P_s and P_c remove double counting that occurs in second order. The spin fluctuations are found to dominate the pairing interaction. The numerical calculations are performed on a square lattice with 256×256 points in the Brillouin zone and with 200 points on the real ω axis up to $16t$ with an almost logarithmic mesh. The full momentum and frequency dependence of the quantities is kept. The convolutions in \mathbf{k} space are carried out using fast Fourier transformation. The superconducting state is found to have $d_{x^2-y^2}$ -wave symmetry. T_c^* is determined from the linearized gap equation.

A field-theoretical derivation of the effective action of phase fluctuations^{8,55,56,57} shows that the phase stiffness for frequency $\omega = 0$ is given by the 3D static superfluid density divided by the effective mass, $n_s(x, T)/m^*$. This quantity is given by

$$\frac{n_s}{m^*} = \frac{2}{\pi e^2} (I_N - I_S) \quad (8)$$

with

$$I_{N,S} = \int_0^{\infty} d\omega \sigma_1^{N,S}(\omega), \quad (9)$$

where σ_1^N (σ_1^S) is the real part of the conductivity in the normal (superconducting) state. Here we utilize the f -sum rule $\int_0^{\infty} d\omega \sigma_1(\omega) = \pi e^2 n / 2m^*$ where n is the 3D electron density. The interpretation of Eq. (8) is that the spectral weight missing from the quasi-particle background in $\sigma(\omega)$ for $T < T_c^*$ must be in the superconducting delta-function peak.

$\sigma(\omega)$ is calculated in the normal and superconducting states using the Kubo formula^{58,59}

$$\begin{aligned} \sigma(\omega) &= \frac{2e^2}{\hbar c} \frac{\pi}{\omega} \int_{-\infty}^{\infty} d\omega' [f(\omega') - f(\omega' + \omega)] \\ &\times \frac{1}{N} \sum_{\mathbf{k}} (v_{\mathbf{k},x}^2 + v_{\mathbf{k},y}^2) [N(\mathbf{k}, \omega' + \omega) N(\mathbf{k}, \omega') \\ &+ A_1(\mathbf{k}, \omega' + \omega) A_1(\mathbf{k}, \omega')], \end{aligned} \quad (10)$$

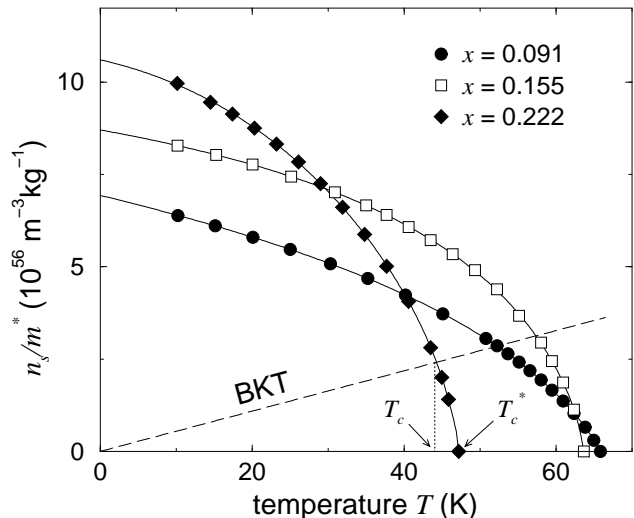


FIG. 1: Static superfluid density as a function of temperature for three values of the doping x (symbols). The solid curves are fits of power laws with logarithmic corrections as explained in the text. The intersection of $n_s(T)/m^*$ with the dashed line represents a simplified criterion for the BKT transition temperature T_c .

where $v_{\mathbf{k},i} = \partial \epsilon_{\mathbf{k}} / \partial k_i$ are the band velocities within the CuO_2 plane and c is the c -axis lattice constant. Vertex corrections are neglected.

The superfluid density (phase stiffness) n_s/m^* obtained in this way is shown in Fig. 1 for the three doping values $x = 0.091$ (underdoped), $x = 0.155$ (approximately optimally doped), and $x = 0.222$ (overdoped). The figure also shows fits to the data at given doping level, where we assume the form $\ln n_s(T)/m^* \cong a_0 + a_1 \ln(T_c^* - T) + a_2 \ln^2(T_c^* - T) + \dots$, *i.e.*, a power-law dependence close to T_c^* with logarithmic corrections. We use the fits to extrapolate to $T = 0$. The results show that T_c^* depends on x only weakly in the underdoped regime but decreases rapidly in the overdoped. We come back to this below. Furthermore, n_s/m^* increases much more slowly below T_c^* in the underdoped regime and extrapolates to a smaller value at $T = 0$.

We have also calculated n_s in units of the total hole density n , shown in Fig. 2, finding that n_s/n is significantly reduced below unity, in agreement with experiments but in contradiction to BCS theory. The reduction is strongest for the underdoped case. Our results show that spin fluctuations can explain most of the observed reduction of n_s . Also note that n_s is linear in temperature for $T \rightarrow 0$ because of the nodes in the gap. The inset in Fig. 2 shows $\lambda^3(0)/\lambda^3(T)$, where the penetration depth is⁷ $\lambda \propto n_s^{-1/2}$, as a function of $T_c^* - T$. The FLEX approximation yields $\lambda^3(0)/\lambda^3(T) \propto T_c^* - T$. The same power law has been found experimentally by Kamal *et al.*⁶⁰ It has been attributed to critical fluctuations starting about 10 K below the transition temperature,⁶⁰ since it coincides with the critical exponent expected for

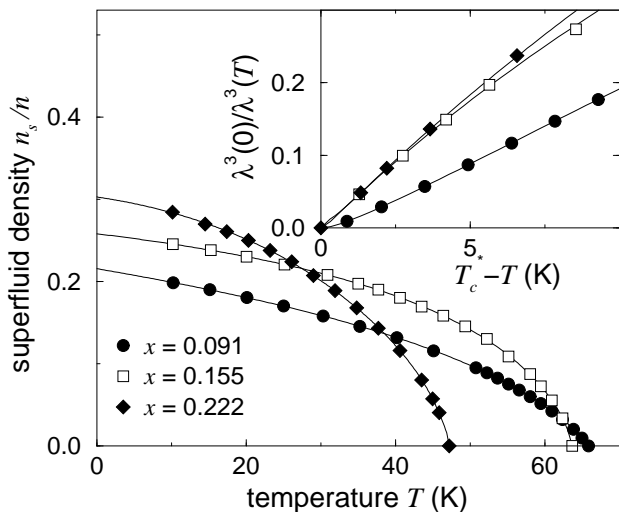


FIG. 2: Ratio of superfluid density to total hole density for the same doping values x as in Fig. 1. The inset shows $\lambda^3(T=0)/\lambda^3(T) = n_s^{3/2}(T)/n_s^{3/2}(T=0)$, where λ is the London penetration depth, as a function of $(T_c^* - T)$.

the 3D XY model. We here obtain *the same* power law from the FLEX approximation, which is purely 2D and does not contain critical fluctuations. Instead this rapid increase of $n_s \propto 1/\lambda^2$ below T_c^* is due to the self-consistency, which leads to a more rapid opening of the gap than in BCS theory. We thus conclude that, while critical 3D XY fluctuations are expected in a narrow temperature range,^{19,20} they are not the origin of the observed power law on the scale of 10 K.

Now we turn to the renormalization of n_s due to phase (vortex) fluctuations. The BKT theory describes the unbinding of thermally created pancake vortex-antivortex pairs.^{21,23} The relevant parameters are the dimensionless stiffness K and the core energy E_c of vortices. The stiffness is related to n_s by⁶¹

$$K(T) = \beta \hbar^2 \frac{n_s(T)}{m^*} \frac{d}{4}, \quad (11)$$

where β is the inverse temperature and d is the average spacing between CuO_2 layers. Since we use a 2D model to describe double-layer cuprates, we set d to half the height of the unit cell of the typical representative $\text{YBa}_2\text{Cu}_3\text{O}_{6+y}$. The stiffness K is also a measure of the strength of the vortex-antivortex interaction $V = 2\pi k_B T K \ln(r/r_0)$. Here, r_0 is the minimum pair size, *i.e.*, twice the vortex core radius, which is of the order of the in-plane Ginzburg-Landau coherence length ξ_{ab} . For the core energy we use an approximate result by Blatter *et al.*,²⁰ $E_c = \pi k_B T K \ln \kappa$, where κ is the Ginzburg parameter. Starting from the smallest vortex-antivortex pairs of size r_0 , the pairs are integrated out and their effect is incorporated by an approximate renormalization of K and the fugacity⁶² $y = e^{-\beta E_c}$. This leads

to the Kosterlitz recursion relations

$$\frac{dy}{dl} = (2 - \pi K) y, \quad (12)$$

$$\frac{dK}{dl} = -4\pi^3 y^2 K^2, \quad (13)$$

where $l = \ln(r/r_0)$ is a logarithmic length scale. For $T > T_c$, K goes to zero for $l \rightarrow \infty$, so that the interaction is screened at large distances and the largest vortex-antivortex pairs unbind. The unbound vortices destroy the superconducting order and the Meißner effect and lead to dissipation.⁶³ For $T < T_c$, K approaches a finite value $K_R \equiv \lim_{l \rightarrow \infty} K$ and y vanishes in the limit $l \rightarrow \infty$ so that there are exponentially few large pairs and they still feel the logarithmic interaction. Bound pairs reduce K and thus n_s , but do not destroy superconductivity. At T_c , K_R jumps from a universal value of $2/\pi$ to zero. The values of T_c shown below are obtained by numerically integrating Eqs. (12) and (13) with n_s taken from an interpolation between the points in Fig. 1. It turns out that the renormalization of K for $T < T_c$ is very small so that one obtains T_c from the simple criterion

$$K(T_c) = \frac{2}{\pi} \quad \text{or} \quad \frac{n_s(T_c)}{m^*} = \frac{2}{\pi} \frac{4k_B T_c}{\hbar^2 d} \quad (14)$$

for the *unrenormalized* stiffness with an error of less than 1%. Eq. (14) is satisfied at the intersection of the $n_s(T)/m^*$ curves with the dashed straight line in Fig. 1.

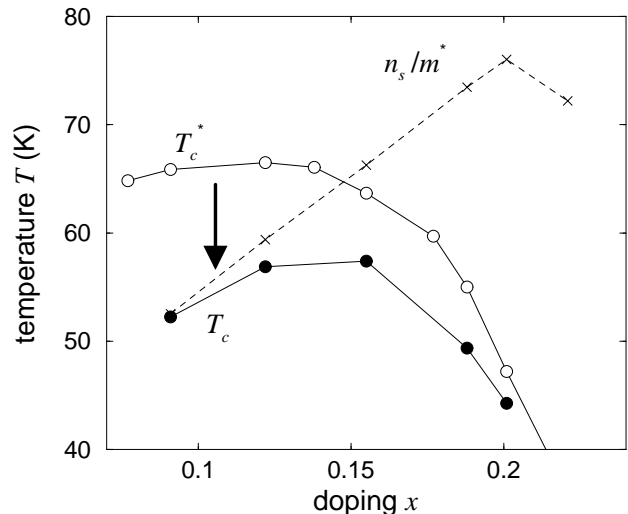


FIG. 3: Temperature scales of the cuprates as functions of doping x . T_c (solid circles) is the transition temperature obtained from the FLEX approximation with phase fluctuations included by means of BKT theory. At T_c^* (open circles) Cooper pairs start to form locally; this temperature is given by the transition temperature obtained from the FLEX approximation with spin fluctuations alone. The crosses show the superfluid density (phase stiffness) $n_s(T=0)/m^*$ for comparison. This curve has been scaled so that it agrees with T_c in the underdoped regime.

From BKT theory we obtain two important quantities: the transition temperature T_c and the renormalized stiffness K_R , which determines the renormalized superfluid density (phase stiffness)

$$\frac{n_s^R}{m^*} = \frac{4}{\beta \hbar^2 d} K_R. \quad (15)$$

In Fig. 3 we plot the transition temperature T_c and the temperature T_c^* where Cooper-pairs form. For decreasing doping x , T_c^* becomes nearly constant and even decreases for the lowest doping level, consistent with the strong decrease of the onset temperature of vortex effects at even lower doping found by Xu *et al.*^{43,44} We have also calculated the superconducting gap Δ_0 extrapolated to $T = 0$ (not shown). Δ_0 is here defined as half the peak-to-peak separation in the density of states. We find approximately $\Delta_0 \propto T_c^*$.

Phase fluctuations lead to a downturn of T_c in the underdoped regime. However, this reduction is not as large as experimentally observed and our value $x \approx 0.14$ for the optimal doping is accordingly smaller than the experimental one of $x \approx 0.16$.⁶⁴ We suggest that one origin of this discrepancy is the neglect of the feedback of phase fluctuations on the electronic properties.

Figure 3 also shows the superfluid density $n_s(0)/m^*$ extrapolated to $T = 0$, scaled such that it approaches T_c in the underdoped regime. The density increases approximately linearly with doping except for the most overdoped point, where it turns down again. This behavior agrees well with angle-resolved photoemission (ARPES) results of Feng *et al.*⁶⁵ and with recent μ SR experiments of Bernhard *et al.*⁶⁶ In Ref. 66 a maximum in n_s at a unique doping value of $x_{\max} \approx 0.19$ is found for various cuprates, while we obtain $x_{\max} \approx 0.20$. Our results are consistent with the Uemura scaling¹ $T_c \propto n_s(0)$ in the heavily underdoped regime and with the BCS-like behavior $T_c \approx T_c^* \propto \Delta_0$ in the overdoped limit. T_c interpolates smoothly between the extreme cases. We find $T_c < T_c^*$ even for high doping, since $n_s(T)$ and $K(T)$ continuously go to zero at T_c^* so that Eq. (14) is only satisfied at a temperature $T_c < T_c^*$. The results for the overdoped case may be changed if amplitude fluctuations of the order parameter and their mixing with phase fluctuations⁶⁷ are taken into account. Amplitude fluctuations are governed by Δ , which becomes smaller than the energy scale of phase fluctuations in the overdoped regime.

The situation is complicated by the Josephson coupling between CuO_2 layers. This coupling leads to the appearance of Josephson vortex lines connecting the pancake vortices between the layers.²⁰ They induce a *linear* component in the vortex-antivortex interaction. This contribution becomes relevant at separations larger than $\Lambda = d/\epsilon$, where $\epsilon < 1$ is the anisotropy parameter.²⁰ Λ acts as a cutoff for the Kosterlitz recursion relations and eventually leads to an increase of T_c relative to the BKT result T_c^{BKT} and to the breakdown of 2D theory close to the transition.^{20,25,26,27} The experiments of Corson *et al.*⁴¹ also show that the BKT temperature T_c^{BKT}

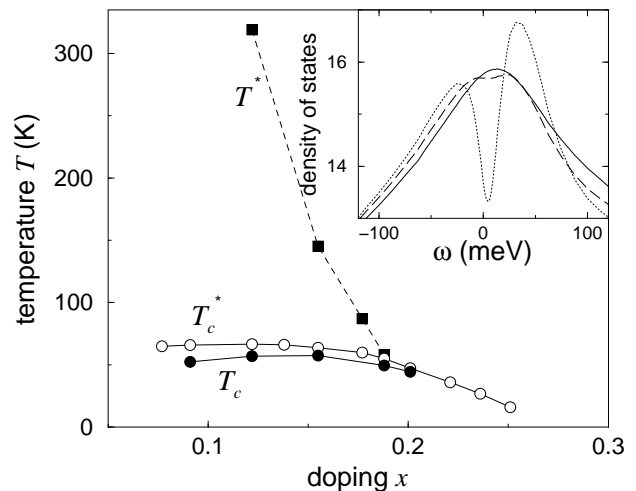


FIG. 4: Temperature T^* at which a small suppression of the density of states at the Fermi energy (weak pseudogap) appears. The temperatures T_c^* and T_c from Fig. 3 are also shown. The inset shows the suppression of the density of states (in arbitrary units) for $x = 0.155$ and $T = 4.5 T_c^*$ (solid line), $T = 2.3 T_c^* \approx T^*$ (dashed line), and $T = 1.01 T_c^*$ (dotted line).

extracted from the data is significantly smaller than the experimental T_c . Thus T_c as calculated here is a lower bound of the true transition temperature.

The feedback of phase fluctuations on the electrons is not included in our approach. We expect the phase fluctuations in this regime to lead to pair breaking.⁸ However, simulations of the XY model suggest that this feedback is rather weak.⁶⁸ Neglecting the feedback, the electronic spectral function shows the unrenormalized superconducting gap for $T_c < T < T_c^*$. Since there is no superconducting order in this regime, we identify this gap with the (strong) pseudogap, which thus is automatically $d_{x^2-y^2}$ -wave-like and of the same magnitude as the superconducting gap for $T < T_c$. Thus in this picture the pseudogap is due to local Cooper pair formation in the absence of long-range phase coherence. Pair breaking due to phase fluctuations should partly fill in this gap.

Figure 4 shows T_c , T_c^* , and T^* on a different temperature scale. T^* is the highest temperature where a weak pseudogap is obtained from FLEX, *i.e.*, where the density of states at the Fermi energy starts to be suppressed. The inset shows this suppression for $x = 0.155$. The temperature T^* becomes much larger than T_c in the underdoped regime, in agreement with experiments.¹⁵

To conclude this section, we discuss the effect of a normal-state pseudogap due to a mechanism other than incoherent Cooper pairing. Let us assume a suppression of the density of states close to the Fermi surface in the normal state, *e.g.*, due to the formation of a charge-density wave.⁷¹ This decreases the number of holes available for pairing and should thus reduce T_c . To check this, we have performed FLEX calculations with a pseu-

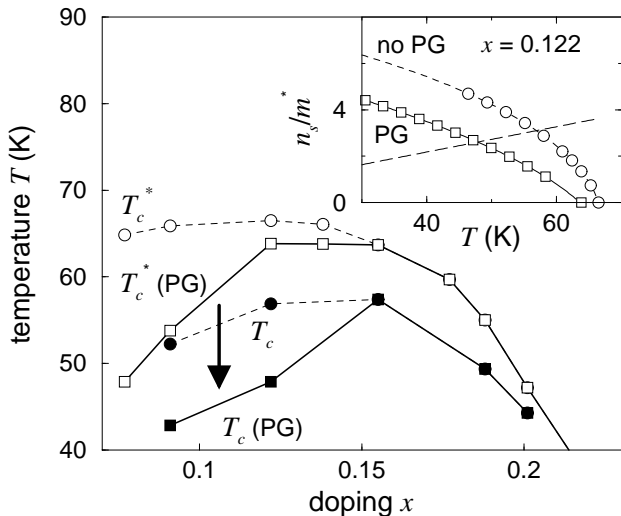


FIG. 5: Transition temperatures in the presence of a normal-state pseudogap. The open squares show the transition temperature T_c^* obtained from the FLEX approximation with a d -wave pseudogap in the normal-state dispersion. The amplitude of the pseudogap is taken from experiments.^{69,70} The open circles show the corresponding values without a pseudogap, see Fig. 3. The solid squares denote T_c in the presence of the pseudogap and with phase fluctuations included, assuming the two effects to be independent. The solid circles show the corresponding results without pseudogap. The inset gives the phase stiffness n_s/m^* for the doping $x = 0.122$ with (lower curve) and without (upper curve) the pseudogap. Intersections with the dashed line give the simple criterion (14) for T_c . One clearly sees that a normal-state pseudogap increases the effect of phase fluctuations due to the slow increase of n_s/m^* below T_c^* .

dogap of the form $\Delta_{\mathbf{k}} = \Delta_0 (\cos k_x - \cos k_y)$ included in the normal-state dispersion. The doping-dependent amplitude Δ_0 is chosen in accordance with ARPES experiments by Marshall *et al.*⁶⁹ and by Ding *et al.*⁷⁰ The results are shown by the open squares in Fig. 5. The curve merges with the T_c^* curve without pseudogap (open circles) at $x = 0.155$, since here the pseudogap is experimentally found to vanish.^{69,70} It is apparent that T_c^* is indeed strongly reduced in the underdoped regime. Thus this density-of-states effect is a possible alternative explanation for the observed downturn of T_c .

Next, we consider phase fluctuations in the presence of a normal-state pseudogap. The T_c values naively obtained from BKT theory for this case are shown in Fig. 5 as the solid squares. Phase fluctuations reduce T_c even more, in particular for $x = 0.122$. This is due to the fact that the phase stiffness n_s/m^* increases much more slowly below T_c^* in the presence of a pseudogap, as shown in the inset of Fig. 5, even if T_c^* is only slightly reduced. The small stiffness makes phase fluctuations more effective. However, in this picture the reduction of T_c is probably overestimated: Above, we have explained the pseudogap as resulting from incoherent Cooper pairing. This

contribution to the pseudogap must *not* be incorporated into the normal-state dispersion to avoid double counting. This would increase the result for T_c . It is clearly important to develop a theory that incorporates phase fluctuations, spin fluctuations, and possibly the charge-density wave on the same microscopic level. However, the inclusion of vortex fluctuations in a FLEX-type theory on equal footing with spin fluctuations would be a formidable task.⁸

III. DYNAMICAL CASE

In this section, we calculate the *dynamical* phase stiffness, which is the quantity obtained by Corson *et al.*⁴¹ We first note that the superfluid density can also be obtained from the imaginary part of the conductivity,

$$\frac{n_s}{m^*} = \frac{1}{e^2} \lim_{\omega \rightarrow 0} \omega \sigma_2^S(\omega), \quad (16)$$

as can be shown with the help of Kramers-Kronig relations. We have recalculated n_s/m^* in this way and find identical results compared to Eq. (8).

The phase stiffness has also been obtained at nonzero frequencies using field-theoretical methods.^{8,55,56,57} For small wave vector $\mathbf{q} \rightarrow 0$,

$$\frac{n_s(\omega)}{m^*} = \frac{1}{e^2} \omega \sigma_2^S(\omega). \quad (17)$$

The imaginary part $\sigma_2^S(\omega)$ of the dynamical conductivity is obtained from the FLEX approximation for the dynamical current-current correlation function using the Kubo formula.⁵⁸ For $\omega > 0$ one should not interpret $n_s(\omega)$ as a density. Note also that $n_s^{-1/2}(\omega)$ is no longer proportional to the penetration depth of a magnetic field—for $\omega > 0$ there is also a contribution from the *real* part of the conductivity, *i.e.*, the normal skin effect.

The resulting phase stiffness $n_s(\omega)/m^*$ is shown in Fig. 6 for $x = 0.122$ (underdoped) at various temperatures. At higher doping the results (not shown) are similar, only the typical frequency scale, which turns out to be the low-temperature superconducting gap Δ_0 , is reduced. We find a finite phase stiffness at $\omega > 0$ even for $T \geq T_c^*$. At first glance this is surprising, since the phase is not well-defined for $\Delta = 0$. Indeed, using a Ward identity one can show that the Gaussian part of the phase action vanishes for $T \geq T_c^*$.⁷² However, the phase action contains a contribution from the time derivative of the phase besides the stiffness term. While the total action vanishes, each term on its own does not. Thus the stiffness is finite but has no physical significance for $T \geq T_c^*$.

Even slightly below T_c^* , $n_s(\omega = 0)/m^*$ obtains a significant finite value, leading to the Meißner effect, and there is a considerable redistribution of weight from energies roughly above twice the low-temperature maximum gap, $2\Delta_0$, to energies below $2\Delta_0$. This redistribution increases with decreasing temperature. Also, a peak develops slightly below Δ_0 followed by a dip around $2\Delta_0$, this

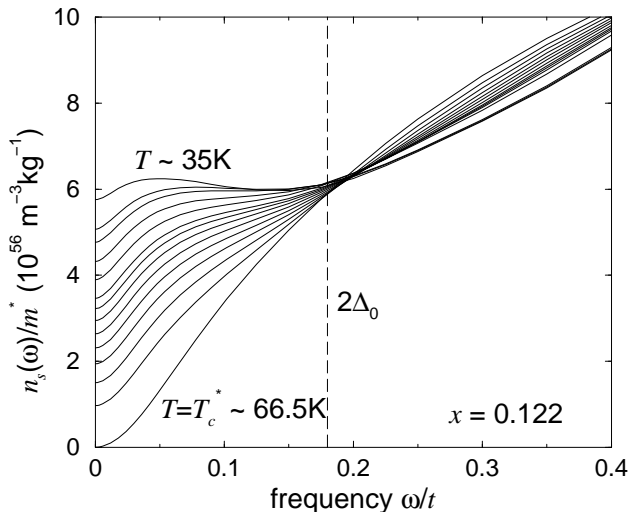


FIG. 6: Frequency-dependent phase stiffness $n_s(\omega)/m^*$ for doping $x = 0.122$ (underdoped) and temperatures $k_B T/t = 0.012, 0.015, 0.016, 0.017, 0.018, 0.019, 0.0195, 0.02, 0.0205, 0.021, 0.0215, 0.022, 0.0225, 0.023$ [with decreasing $n_s(0)/m^*$]. $t = 250$ meV is the hopping integral. The frequency is given in units of t ($\hbar = 1$). At $T_c^* \approx 0.023 t/k_B = 66.5$ K Cooper pairs start to form. Below T_c^* there is a marked transfer of weight from energies above $2\Delta_0$ to energies below, where Δ_0 is the maximum gap at low temperatures as obtained from the FLEX approximation.

structure being most pronounced in the underdoped case. Since Δ_0 is smaller in the overdoped regime, $n_s(\omega)/m^*$ changes more rapidly for small ω in this case. It is of course not surprising that $2\Delta_0$ is the characteristic frequency of changes in $n_s(\omega)/m^*$ related to the formation of Cooper pairs.

We now turn to the question of how phase fluctuations affect the dynamical phase stiffness $n_s(\omega)/m^*$. This requires a dynamical generalization of BKT theory, which was first developed by Ambegaokar *et al.*^{23,42} Here, we start from a heuristic argument for the dynamical screening of the vortex interaction:⁴² An applied electromagnetic field exerts a force on the vortices mainly by inducing a superflow, which leads to a Lorentz force on the flux carried by the vortices. On the other hand, moving a vortex leads to dissipation in its core and thus to a finite diffusion constant D_v ,⁷³ which impedes its motion. If one assumes a rotating field of frequency ω , small vortex-antivortex pairs will rotate to stay aligned with the field. Large pairs, on the other hand, will not be able to follow the rotation and thus become ineffective for the screening. A pair can follow the field if its component vortex and antivortex can move a distance $2\pi r$ during one period $T_\omega = 2\pi/\omega$. During this time a vortex can move a distance of about the diffusion length $\sqrt{D_v T_\omega} = \sqrt{2\pi D_v/\omega}$, so that the critical scale for the pair size is

$$r_\omega \equiv \sqrt{\frac{D_v}{2\pi\omega}}. \quad (18)$$

Only vortex-antivortex pairs of size $r \lesssim r_\omega$ contribute to the screening. Hence, we cut off the renormalization flows at this length scale. To avoid an unphysical kink in $n_s^R(\omega)/m^*$ we use the smooth cutoff $\bar{r}^2 = r_\omega^2 + r_0^2$.

The diffusion constant of vortices is not easy to calculate accurately. In the absence of pinning, the theory of Bardeen and Stephen⁷³ yields

$$D_v^0 = \frac{2\pi c^2 \xi_{ab}^2 \rho_n k_B T}{\phi_0^2 \tilde{d}}, \quad (19)$$

where c is the speed of light, $\xi_{ab} \sim r_0/2$ is the coherence length, ρ_n is the normal-state resistivity, $\phi_0 = hc/2e$ is the superconducting flux quantum, and \tilde{d} is an effective layer thickness. In the renormalization the quantity D_v^0/r_0^2 enters, which according to Eq. (19) is linear in temperature. In the presence of a high density of weak pinning centers the diffusion constant becomes⁷⁴ $D_v = D_v^0 \exp(-E_p/k_B T)$, where E_p is the pinning energy. Matters are complicated by the observation that E_p depends on temperature. Rogers *et al.*⁷⁵ find $E_p(T) \approx E_p^0(1 - T/T_c^*)$ with $E_p^0/k_B \approx 1200$ K for $\text{Bi}_2\text{Sr}_2\text{CaCu}_2\text{O}_{8+\delta}$. Absorbing the constant term in the exponent into the prefactor, the result for the diffusion constant in natural units is

$$\frac{D_v}{r_0^2} \approx C_v \frac{k_B T}{\hbar} \exp\left(-\frac{E_p^0}{k_B T}\right), \quad (20)$$

where C_v is a dimensionless constant. However, such a large value of E_p^0 would lead to a sharp, step-like dependence of $n_s(\omega)/m^*$ on temperature, in contradiction to the smooth behavior shown in Fig. 4 of Ref. 41. In view of these difficulties we treat D_v/r_0^2 as a constant parameter and discuss the dependence on D_v below.

To find the effect of phase (vortex) fluctuations on the phase stiffness, the recursion relations (12) and (13) are now integrated numerically up to the cutoff $\bar{l} = \ln(\bar{r}/r_0)$, which depends on D_v/r_0^2 . The resulting renormalized phase stiffness $n_s^R(\omega)/m^*$ for constant $D_v/r_0^2 = 10^{17} \text{ s}^{-1}$ and $x = 0.122$ is plotted in Fig. 7. Other values of D_v give similar results. Of course, faster vortex diffusion shifts the features at given temperature to higher frequencies. The dashed lines denote the unrenormalized stiffness, *i.e.*, the same data as in Fig. 6, albeit on an expanded frequency scale. The highest frequency used in Ref. 41 (600 GHz) corresponds to $\omega/t \approx 0.01$, also indicated in Fig. 7.

For $T < T_c$ (the upper six curves) the static renormalization has been found to be small, see Sec. II. The renormalization at finite ω is even weaker so that the renormalized stiffness is in practice identical to the unrenormalized one, which has only a weak frequency dependence for low ω , in agreement with Ref. 41.

When T is increased above T_c (the lower five curves in Fig. 7), a strong renormalization of the stiffness due to phase fluctuations sets in starting at very low frequencies. The Meißner effect is thus destroyed for all $T > T_c$ by

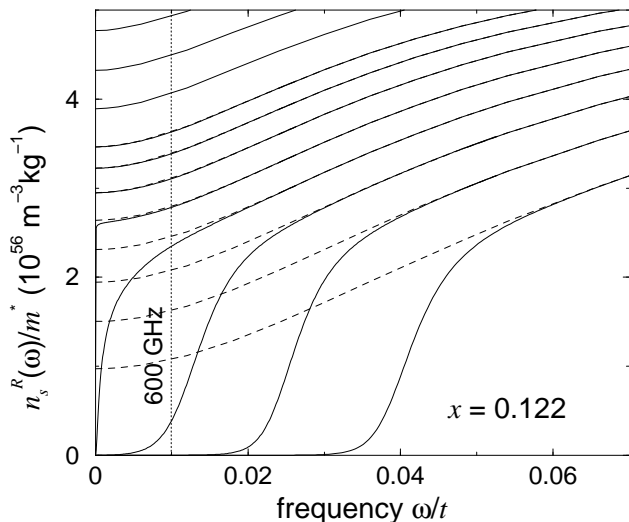


FIG. 7: Phase stiffness $n_s^R(\omega)/m^*$ renormalized by vortex fluctuations for $x = 0.122$ at temperatures $k_B T/t = 0.016, 0.017, 0.018, 0.019, 0.0195, 0.02, 0.0205, 0.021, 0.0215, 0.022, 0.0225$ (heavy solid lines). The vortex diffusion constant has been chosen as $D_v/r_0^2 = 10^{17} \text{ s}^{-1}$. The unrenormalized stiffness is shown as dashed lines; these are the same data as in Fig. 6. Note the expanded frequency scale. The highest frequency used by Corson *et al.*⁴¹ is indicated by the vertical dotted line.

the comparatively slow vortex diffusion. With increasing temperature the onset of renormalization shifts to higher frequencies. At frequencies above this onset, the vortices cannot follow the field and thus do not affect the response, as discussed above. The onset frequencies are always much smaller than $2\Delta_0$. The features at the energy scale $2\Delta_0$ shown in Fig. 6, which are due to Cooper-pair formation, are unaffected by phase fluctuations and show no anomaly at T_c . They vanish only at T_c^* .

Finally, in Fig. 8 we plot the renormalized $n_s^R(\omega)/m^*$ for $x = 0.122$ as a function of temperature for various frequencies. This graph should be compared to Figs. 2 and 4 of Ref. 41—note that the quantity T_θ given there is proportional to n_s^R/m^* . We note that Corson *et al.*⁴¹ assume a thermally activated density of free vortices, $n_f \propto \exp(-E_f/T)$, for T not too close to the BKT transition temperature, and a temperature-independent diffusion constant.⁷⁶ Here, we instead integrate the recursion relations (12) and (13) explicitly up to the dynamical length scale \bar{r} so that we do not have to make an assumption on n_f . One sees that even at $f = 600$ GHz the broadened BKT transition is still much narrower than found by Corson *et al.*⁴¹ From Eqs. (19) and (20) it is clear that the diffusion constant D_v/r_0^2 increases with temperature. In the presence of pinning it increases rapidly around $k_B T \sim E_p^0$. Since a larger diffusion constant, *i.e.*, more mobile vortices, leads to stronger renormalization, the transition in Fig. 8 would become *even sharper* if D_v/r_0^2 were an increasing function of temperature.

Our results show that dynamical BKT theory together

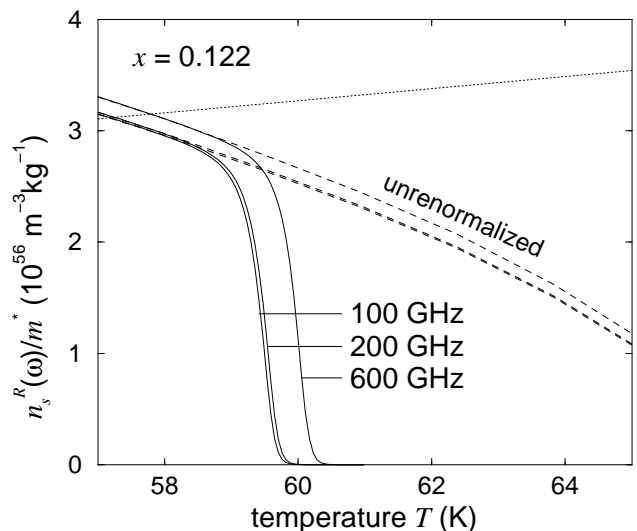


FIG. 8: Renormalized phase stiffness $n_s^R(\omega)/m^*$ for $x = 0.122$ as a function of temperature for frequencies $f = 100$ GHz, 200 GHz, 600 GHz (heavy solid lines). The unrenormalized stiffness is shown as dashed lines. The dotted line represents the approximate criterion Eq. (14) for the ($\omega = 0$) BKT transition.

with Bardeen-Stephen theory for vortex diffusion and natural assumptions on pinning does *not* agree quantitatively with the experimental results.⁴¹ We conclude that the finite size effect apparent in the experimental data is not only due to the finite diffusion length. Another possible source is the interlayer Josephson coupling, which leads to the appearance of the Josephson length Λ as an additional length scale, as discussed above.²⁰ This length scale leads to a cutoff of the recursion relations at $l \sim \ln(\Lambda/r_0)$, which becomes small close to T_c^* due to the divergence of $r_0 \sim \xi_{ab}$ (neglecting the feedback of phase fluctuations on the quasiparticles). This broadens the transition but cannot easily explain the observed frequency dependence. On the other hand, the experimental observation that the curves for various frequencies⁴¹ start to coincide where the phase stiffness agrees with the universal jump criterion (14) supports an interpretation in terms of vortex fluctuations. We suggest that a better description of the interplay of vortex dynamics and interlayer coupling is required to understand the data.

Note, the origin of the discrepancy may also lie in the FLEX results for $n_s(\omega)/m^*$, which do not include all effects of temperature-dependent scattering on the conductivity σ ,⁷⁷ and in the omission of the feedback of phase fluctuations on the electronic properties. Another effect neglected here is the possible coupling to a charge-density wave perhaps taking the form of dynamical stripes.

IV. SUMMARY AND CONCLUSIONS

In the present paper we have obtained the characteristic energy scales of hole-doped cuprate superconductors from a theory that includes both spin and Cooper-pair phase fluctuations. The former are described by the FLEX approximation, whereas the latter are included by means of the Berezinskii-Kosterlitz-Thouless (BKT) theory, taking the FLEX results as input. Phase fluctuations mainly take the form of *vortex* fluctuations, since Gaussian phase fluctuations have a large energy gap. Vortices lead to the renormalization of the phase stiffness $n_s(\omega)/m^*$ to $n_s^R(\omega)/m^*$. The stiffness at $T \rightarrow 0$ shows a maximum at a doping level of $x \approx 0.2$, in good agreement with experiments.⁶⁶ At the transition temperature T_c the renormalized static phase stiffness $n_s^R(\omega = 0)/m^*$ vanishes, leading to the disappearance of the Meißner effect. The ideal conductivity is also destroyed by free vortices. T_c is significantly reduced compared to the transition temperature T_c^* that would result from spin fluctuations alone. The T_c determined from spin *and* phase (vortex) fluctuations is in much better agreement with experiments in the underdoped regime and shows a maximum at optimum doping. Still, our approach does not explain the full reduction of T_c . We believe that a further reduction of T_c results from (a) the breaking of Cooper pairs by scattering with phase fluctuations and (b) other instabilities that reduce the density of states in the normal state, for example a charge-density wave. Since the latter effect also suppresses n_s/m^* , phase fluctuations

can become even more effective and reduce T_c further. It would be desirable to include the pair-breaking effect of phase fluctuations and the possible formation of a charge-density wave on the same microscopic level as the spin fluctuations.⁸

For $T_c < T < T_c^*$, where phase-coherent superconductivity is absent, phase fluctuations lead to a strong renormalization of n_s/m^* at frequencies much smaller than $2\Delta_0$. Our results show the same trends as found in conductivity measurements.⁴¹ However, a three-dimensional description of vortex dynamics might be required to obtain a more quantitative agreement. Local formation of Cooper pairs still takes place in this regime. This leads to a strong pseudogap of the same magnitude Δ_0 and symmetry as the superconducting gap below T_c . We also find a frequency dependence of $n_s^R(\omega)/m^*$ at higher frequencies, $\omega \gtrsim \Delta_0$, that is very similar to the superconducting phase. These features vanish only around T_c^* . Finally, for $T_c^* < T < T^*$ there is a weak suppression in the density of states at the Fermi energy. Our results reproduce several of the main features common to all hole-doped cuprate superconductors. We conclude that the exchange of spin fluctuations, modified by strong superconducting phase (vortex) fluctuations in the underdoped regime, is the main mechanism of superconductivity in cuprates.

Acknowledgments

We would like to thank I. Eremin, H. Kleinert, F. Schäfer, and D. Straub for helpful discussions.

* Electronic address: timm@physik.fu-berlin.de

¹ Y. J. Uemura, G. M. Luke, B. J. Sternlieb, J. H. Brewer, J. F. Carolan, W. N. Hardy, R. Kadono, J. R. Kempton, R. F. Kiefl, S. R. Kreitzman, P. Mulhern, T. M. Rise-man, D. Li. Williams, B. X. Yang, S. Uchida, H. Takagi, J. Gopalakrishnan, A. W. Sleight, M. A. Subramanian, C. L. Chien, M. Z. Cieplak, G. Xiao, V. Y. Lee, B. W. Statt, C. E. Stronach, W. J. Kossler, and X. H. Yu, Phys. Rev. Lett. **62**, 2317 (1989).

² C. C. Tsuei, J. R. Kirtley, C. C. Chi, L. S. Yu-Jahnes, A. Gupta, T. Shaw, J. Z. Sun, and M. B. Ketchen, Phys. Rev. Lett. **73**, 593 (1994); J. R. Kirtley, C. C. Tsuei, M. Rupp, J. Z. Sun, L. S. Yu-Jahnes, A. Gupta, M. B. Ketchen, K. A. Moler, and M. Bhushan, *ibid.* **76**, 1336 (1996).

³ J. M. Tranquada, B. J. Sternlieb, J. D. Axe, Y. Nakamura, and S. Uchida, Nature **375**, 561 (1995); P. Dai, H. A. Mook, and F. Dogan, Phys. Rev. Lett. **80**, 1738 (1998); Z.-X. Shen, P. J. White, D. L. Feng, C. Kim, G. D. Gu, H. Ikeda, R. Yoshizaki, and N. Koshizuka, Science **280**, 259 (1998).

⁴ S. Doniach and M. Inui, Phys. Rev. B **41**, 6668 (1990).

⁵ B. K. Chakraverty, A. Taraphder, and M. Avignon, Physica C **235–240**, 2323 (1994).

⁶ V. J. Emery and S. A. Kivelson, Nature **374**, 434 (1995).

⁷ J. R. Schrieffer, *Theory of Superconductivity* (Benjamin, New York, 1964).

⁸ F. Schäfer, C. Timm, D. Manske, and K. H. Bennemann, J. Low Temp. Phys. **117**, 223 (1999); F. Schäfer (unpublished).

⁹ J. Schmalian, S. Grabowski, and K. H. Bennemann, Phys. Rev. B **56**, R509 (1997).

¹⁰ C. Meingast, V. Pasler, P. Nagel, A. Rykov, S. Tajima, and P. Olsson, Phys. Rev. Lett. **86**, 1606 (2001).

¹¹ W. W. Warren, Jr., R. E. Walstedt, G. F. Brennert, R. J. Cava, R. Tycko, R. F. Bell, and G. Dabbagh, Phys. Rev. Lett. **62**, 1193 (1989).

¹² H. J. Tao, F. Lu, and E. J. Wolf, Physica C **282–287**, 1507 (1997); C. Renner, B. Revaz, J.-Y. Genoud, K. Kadowaki, and Ø. Fischer, Phys. Rev. Lett. **80**, 149 (1998).

¹³ H. Takagi, B. Batlogg, H. L. Kao, J. Kwo, R. J. Cava, J. J. Krajewski, and W. F. Peck, Jr., Phys. Rev. Lett. **69**, 2975 (1992).

¹⁴ D. N. Basov and T. Timusk, in *Handbook on the Physics and Chemistry of Rare Earths*, edited by K. A. Dschneider, L. Eyring, and M. B. Maple (North-Holland, Amsterdam, 1999), and references therein.

¹⁵ T. Timusk and B. W. Statt, Rep. Prog. Phys. **62**, 61 (1999), and references therein.

¹⁶ B. Batlogg and V. J. Emery, Nature **382**, 20 (1996); V. J. Emery, S. A. Kivelson, and O. Zachar, Phys. Rev. B **56**, 6120 (1997).

¹⁷ R. S. Markiewicz, cond-mat/0108075.

- ¹⁸ D. Matthey, S. Gariglio, B. Giovannini, and J.-M. Triscone, Phys. Rev. B **64**, 024513 (2001).
- ¹⁹ M. V. Feigel'man, Zh. Eksp. Teor. Fiz. **76**, 784 [Sov. Phys. JETP **49**, 395 (1979)].
- ²⁰ G. Blatter, M. V. Feigel'man, V. B. Geshkenbein, A. I. Larkin, and V. M. Vinokur, Rev. Mod. Phys. **66**, 1125 (1994).
- ²¹ V. L. Berezinskii, Zh. Eksp. Teor. Fiz. **61**, 1144 (1971) [Sov. Phys. JETP **34**, 610 (1972)]; J. M. Kosterlitz and D. J. Thouless, J. Phys. C **6**, 1181 (1973); J. M. Kosterlitz, *ibid.* **7**, 1046 (1974).
- ²² M. R. Beasley, J. E. Mooij, and T. P. Orlando, Phys. Rev. Lett. **42**, 1165 (1979); S. Doniach and B. A. Huberman, Phys. Rev. Lett. **42**, 1169 (1979); B. I. Halperin and D. R. Nelson, J. Low Temp. Phys. **36**, 599 (1979); L. A. Turkevich, J. Phys. C **12**, L385 (1979).
- ²³ P. Minnhagen, Rev. Mod. Phys. **59**, 1001 (1987).
- ²⁴ A. Kovner and B. Rosenstein, Phys. Rev. B **42**, 4748 (1990).
- ²⁵ S. W. Pierson, Phys. Rev. Lett. **73**, 2496 (1994); **75**, 4674 (1995); Phys. Rev. B **51**, 6663 (1995).
- ²⁶ M. Friesen, Phys. Rev. B **51**, 632 (1995).
- ²⁷ C. Timm, Phys. Rev. B **52**, 9751 (1995).
- ²⁸ C. Timm, Phys. Rev. B **55**, 3241 (1997).
- ²⁹ S. W. Pierson, M. Friesen, S. M. Ammirata, J. C. Hunnicutt, and L. A. Gorham, Phys. Rev. B **60**, 1309 (1999); S. W. Pierson and O. T. Valls, Phys. Rev. B **61**, 663 (2000).
- ³⁰ D. Fay, J. Appel, C. Timm, and A. Zabel, Phys. Rev. B **63**, 064509 (2001).
- ³¹ J. H. Schön, M. Dorget, F. C. Beuran, X. Z. Zu, E. Arushanov, C. Deville Cavellin, and M. Laguès, Nature **414**, 434 (2001).
- ³² In 2D Gaussian fluctuations destroy long-range order. However, the transition between quasi-long-range and short-range order still takes place at the mean-field T_c if only Gaussian fluctuations are taken into account.
- ³³ P. W. Anderson, Phys. Rev. **112**, 1900 (1958).
- ³⁴ A. Buzdin and D. Feinberg, J. Phys. France **51**, 1971 (1990); J. R. Clem, Phys. Rev. B **43**, 7837 (1991).
- ³⁵ P. C. E. Stamp, L. Forro, and C. Ayache, Phys. Rev. B **38**, 2847 (1988).
- ³⁶ S. N. Artemenko, I. G. Gorlova, and Y. I. Latyshev, Phys. Lett. A **138**, 428 (1989).
- ³⁷ S. Martin, A. T. Fiory, R. M. Fleming, G. P. Espinosa, and A. S. Cooper, Phys. Rev. Lett. **62**, 677 (1989).
- ³⁸ N. C. Yeh and C. C. Tsuei, Phys. Rev. B **39**, 9708 (1989).
- ³⁹ T. Freltoft, H. J. Jensen, and P. Minnhagen, Solid State Comm. **78**, 635 (1991).
- ⁴⁰ A. K. Pradhan, S. J. Hazell, J. W. Hodby, C. Chen, Y. Hu, and B. M. Wranglyn, Phys. Rev. B **47**, 11374 (1993).
- ⁴¹ J. Corson, R. Mallozzi, J. Orenstein, J. N. Eckstein, and I. Bozovic, Nature **398**, 221 (1999).
- ⁴² V. Ambegaokar, B. I. Halperin, D. R. Nelson, and E. D. Siggia, Phys. Rev. Lett. **40**, 783 (1978); V. Ambegaokar and S. Teitel, Phys. Rev. B **19**, 1667 (1979); V. Ambegaokar, B. I. Halperin, D. R. Nelson, and E. D. Siggia, Phys. Rev. B **21**, 1806 (1980).
- ⁴³ Z. A. Xu, N. P. Ong, Y. Wang, T. Kakeshita, and S. Uchida, Nature **406**, 486 (2000); see also P. A. Lee, *ibid.*, p. 467.
- ⁴⁴ Y. Wang, Z. A. Xu, T. Kakeshita, S. Uchida, S. Ono, Y. Ando, and N. P. Ong, Phys. Rev. B **64**, 224519 (2001).
- ⁴⁵ N. E. Bickers, D. J. Scalapino, and S. R. White, Phys. Rev. Lett. **62**, 961 (1989); N. E. Bickers and D. J. Scalapino, Ann. Phys. (New York) **193**, 206 (1989).
- ⁴⁶ C.-H. Pao and N. E. Bickers, Phys. Rev. Lett. **72**, 1870 (1994); Phys. Rev. B **51**, 16310 (1995).
- ⁴⁷ P. Monthoux and D. J. Scalapino, Phys. Rev. Lett. **72**, 1874 (1994).
- ⁴⁸ T. Dahm and L. Tewordt, Phys. Rev. Lett. **74**, 793 (1995).
- ⁴⁹ M. Langer, J. Schmalian, S. Grabowski, and K. H. Bennemann, Phys. Rev. Lett. **75**, 4508 (1995); S. Grabowski, M. Langer, J. Schmalian, and K. H. Bennemann, Europhys. Lett. **34**, 219 (1996); J. Schmalian, M. Langer, S. Grabowski, and K. H. Bennemann, Comp. Phys. Comm. **93**, 141 (1996).
- ⁵⁰ P. W. Anderson, Science **235**, 1196 (1987); G. Baskaran, Z. Zou, and P. W. Anderson, Sol. State Commun. **63**, 973 (1987); P. W. Anderson, cond-mat/0201429.
- ⁵¹ G. Baym and L.P. Kadanoff, Phys. Rev. **124**, 287 (1961); G. Baym, Phys. Rev. **127**, 1391 (1962).
- ⁵² L. Tewordt, J. Low Temp. Phys. **15**, 349 (1974).
- ⁵³ N. F. Berk and J. R. Schrieffer, Phys. Rev. Lett. **17**, 433 (1966).
- ⁵⁴ Y. Nambu, Phys. Rev. **117**, 648 (1960).
- ⁵⁵ H.-J. Kwon and A. T. Dorsey, Phys. Rev. B **59**, 6438 (1999).
- ⁵⁶ S. G. Sharapov, H. Beck, and V. M. Loktev, Phys. Rev. B **64**, 134519 (2001).
- ⁵⁷ This derivation^{8,55,56} starts from an attractive pairing interaction, which is decoupled using a Hubbard-Stratonovich transformation. The decoupling field is the complex superconducting gap Δ . A gauge transformation of the fermions then removes the phase from Δ and couples it directly to the fermions. After the fermions are integrated out, one obtains the effective action of the phase.
- ⁵⁸ G. D. Mahan, *Many-Particle Physics*, 2nd edition (Plenum, New York, 1990).
- ⁵⁹ S. Wermbter and L. Tewordt, Physica C **211**, 132 (1993).
- ⁶⁰ S. Kamal, D. A. Bonn, N. Goldenfeld, P. J. Hirschfeld, R. Liang, and W. N. Hardy, Phys. Rev. Lett. **73**, 1845 (1994); S. Kamal, R. Liang, A. Hosseini, D. A. Bonn, and W. N. Hardy, Phys. Rev. B **58**, R8933 (1998).
- ⁶¹ The quantity V_0 in Ref. 6 is related to K by $K = \beta V_0$.
- ⁶² One usually writes $y = N_0 e^{-\beta E_c}$, where N_0 is a numerical factor of order unity. However, the results depend on N_0 only very weakly, since the renormalization of n_s below T_c is small.
- ⁶³ J. E. Mooij, in *Percolation, Localization, and Superconductivity*, edited by A. M. Goldman and S. A. Wolf (Plenum, New York, 1984), p. 325.
- ⁶⁴ J. L. Tallon, C. Bernhard, H. Shaked, R. L. Hitterman, and J. D. Jorgensen, Phys. Rev. B **51**, 12911 (1995).
- ⁶⁵ D. L. Feng, D. H. Lu, K. M. Shen, C. Kim, H. Eisaki, A. Damascelli, R. Yoshizaki, J.-I. Shimoyama, K. Kishio, G. D. Gu, S. Oh, A. Andrus, J. O'Donnell, J. N. Eckstein, and Z.-X. Shen, Science **289**, 277 (2000).
- ⁶⁶ C. Bernhard, J. L. Tallon, T. Blasius, A. Golnik, and C. Niedermayer, Phys. Rev. Lett. **86**, 1614 (2001).
- ⁶⁷ A. van Otterlo, D. S. Golubev, A. D. Zaikin, and G. Blatter, Eur. Phys. J. B **10**, 131 (1999).
- ⁶⁸ H. Monien, J. Low. Temp. Phys. (to be published), cond-mat/0110178.
- ⁶⁹ D. S. Marshall, D. S. Dessau, A. G. Loeser, C.-H. Park, A. Y. Matsuura, J. N. Eckstein, I. Bozovic, P. Fournier, A. Kapitulnik, W. E. Spicer, and Z.-X. Shen, Phys. Rev. Lett. **76**, 4841 (1996).
- ⁷⁰ H. Ding, T. Yokoya, J. C. Campuzano, T. Takahashi, M.

- Randeria, M. R. Norman, T. Mochiku, K. Kadowaki, and J. Giapintzakis, *Nature* **382**, 51 (1996).
- ⁷¹ T. Dahm, D. Manske, and L. Tewordt, *Phys. Rev. B* **56**, R11419 (1997), and references therein.
- ⁷² C. Timm (unpublished).
- ⁷³ J. Bardeen and M. J. Stephen, *Phys. Rev.* **140**, 1197A (1965).
- ⁷⁴ D. S. Fisher, *Phys. Rev. B* **22**, 1190 (1980).
- ⁷⁵ C. T. Rogers, K. E. Myers, J. N. Eckstein, and I. Bozovic, *Phys. Rev. Lett.* **69**, 160 (1992).
- ⁷⁶ Note that the quantity shown in the inset in Fig. 3 of Ref. 41 is $1/(\Theta\Omega)$ instead of $\Theta\Omega$ and that in the caption one should have $\Omega = (\Omega_0/\Theta) \exp(2C/\Theta)$.
- ⁷⁷ S. Hensen, G. Müller, C. T. Rieck, and K. Scharnberg, *Phys. Rev. B* **56**, 6237 (1997).